1 hour (*15*). Examination of these cells when loaded with fluo-3 after exposure to 10^{-6} M colchicine for 1 hour did not show an increase in the concentration of intracellular Ca^{2+} in either contracting or quiescent cardiocytes (*15*).
33. R. R. Hocking, *The Analysis of Linear Models* (Brooks-Cole, Monterey, CA, 1985), pp. 69–101.

34. We thank S. Prutting, V. Harper, and M. Barnes for technical assistance and J. Lindroth for computer programming. Supported by the Veterans Administration and by the NIH (grant HL37196). G.C. is a VA Clinical Investigator.

29 October 1992; accepted 26 February 1993

Intermediate Filament Formation by a Yeast Protein Essential for Organelle Inheritance

Stephen J. McConnell and Michael P. Yaffe*

Intermediate filaments are abundant cytoskeletal components whose specific cellular functions are poorly understood. The *Saccharomyces cerevisiae* protein MDM1 displays structure and solubility properties that are similar to those of intermediate filament proteins of animal cells. Yeast cells that have a mutant form of MDM1 exhibit temperature-sensitive growth and defective transfer of nuclei and mitochondria to daughter cells during incubation at the nonpermissive temperature of 37°C. The purified, wild-type MDM1 protein readily forms 10-nanometer-wide filaments at either 4°C or 37°C. In contrast, the purified, mutant protein forms filaments at 4°C but fails to form such structures at 37°C. These results suggest that intermediate filament proteins are universal components of eukaryotic cells.

Intermediate filaments have been characterized extensively in higher eukaryotic cells and constitute a prominent system of filaments, 10 nm in diameter, that extend in arrays and networks throughout the cytoplasm (*1*, *2*). The proteins that form these networks share certain conserved structural features and physical properties (*3*–*5*). In addition, purified intermediate filament proteins from a number of sources are able to self-assemble into 10-nm-diameter filaments in vitro in a process independent of energy requirements or cofactors (*5*). Cytoplasmic intermediate filaments have been implicated in a number of roles, including maintaining cellular mechanical stability (*6*) and mediating intracellular communication (*2*), although many details of their dynamics and specific cellular functions are obscure (*1*, *2*, *5*).

The yeast MDM1 protein shares several properties with intermediate filament proteins of animal cells, including a similar solubility profile and similarities of amino acid sequence (*7*). MDM1 was identified through the analysis of a *Saccharomyces cerevisiae* mutant, *mdm1*, that displays temperature-sensitive growth and a failure to transfer nuclei and mitochondria into developing daughter buds during incubation at 37°C (*8*). The wild-type *MDM1* gene was cloned, and its product (MDM1) was shown to be an essential, 51-kD polypeptide (*7*). Antibodies raised against MDM1 recognized a pattern of spots and punctate arrays distributed throughout the yeast cell cytoplasm. In *mdm1* mutant cells, these structures were apparent at 4°C and 23°C but disappeared after *mdm1* mutant cells were shifted to the nonpermissive temperature (*7*). Affinity-purified antibodies against MDM1 also recognized intermediate filaments in indirect immunofluorescence of a variety of animal cells (*7*).

To compare wild-type and mutant forms of MDM1, we cloned and analyzed the mutant gene (*9*). The *mdm1* gene was isolated from mutant yeast by the allelic-marker rescue approach (*10*). The identity of the recovered gene was confirmed by nucleotide sequence analysis (*11*), which revealed a single difference from the wild-type gene: a transition of G to A at nucleotide 770, resulting in a change of Ser^{257} to Asn. When a wild-type copy of *MDM1* was replaced by the recovered mutant *mdm1* gene in intact cells, the original mutant phenotype was generated (*12*).

Both wild-type and mutant MDM1 proteins were produced for further analysis by expression of the genes in bacterial cells (*13*) (Fig. 1A). Purification of wild-type and mutant proteins from bacterial inclusion bodies by differential extraction (*14*) yielded essentially homogeneous preparations (Fig. 1B).

To test the ability of MDM1 to self-assemble into filaments, we dialyzed the purified protein solubilized in 9 M urea against buffers of physiological or low ionic strength (*15*). Protein samples then were examined by electron microscopy on grids after negative staining. Wild-type MDM1 protein readily formed filaments during dialysis against a physiological salt solution (Fig. 2, A through C). Filaments displayed a generally curvilinear, "smooth" appearance (Fig. 2, A through C), with an average diameter of 10.12 ± 0.45 nm (n = 50). Tangled or aggregrated filamentous structures were also apparent on the grids (Fig. 2B). Under the conditions used for filament assembly, 20 to 40% of the purified MDM1 appeared competent for incorporation into filaments or filamentous structures (*16*). Filaments recovered by centrifugation after dialysis or generated by several cycles of solubilization in 9 M urea, reformation by dialysis, and recovery by centrifugation had the same appearance (*12*). Dialysis of urea-solubilized samples at various protein concentrations indicated that MDM1 displays a critical concentration for filament assembly of approximately 50 μg/ml. Individual filaments or filamentous aggregrates failed to form upon dialysis of MDM1 against a buffer of low ionic strength (Fig. 2D). These results demonstrate that the MDM1 protein can self-assemble into 10-nm-wide filaments in the absence of high-energy compounds or other cofactors.

The wild-type MDM1 protein was found to form filaments during dialysis at either 4°C (Fig. 3A) or 37°C (Fig. 3B). Filaments assembled at either temperature appeared equivalent and formed with approximately the same critical concentration for assembly. The purified, mutant MDM1 protein, encoded by the *mdm1* gene, also formed 10-nm-wide filaments at 4°C (Fig. 3C). These filaments were essentially identical to those formed by the wild-type protein. The

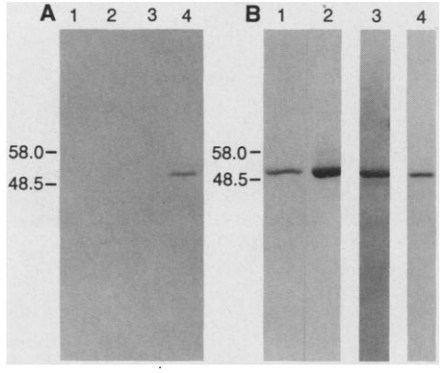

Fig. 1. Expression and purification of MDM1. (**A**) Immunoblot of MDM1 in protein extracts of bacterial cells that had a control vector, pET11-a (lanes 1 and 2), or a vector encoding *MDM1*, pET11-a-*MDM1* (lanes 3 and 4). Cells were uninduced (lanes 1 and 3) or induced with isopropyl-1-thio-β-D-galactoside (lanes 2 and 4). (**B**) Analysis of purified MDM1. Lane 1, wild-type MDM1 protein (5 μg) stained with Coomassie blue; lane 2, wild-type MDM1 protein (30 μg) stained with Coomassie blue; lane 3, mutant MDM1 protein (7 μg) stained with Coomassie blue; lane 4, immunoblot analysis of wild-type MDM1 (100 ng). Molecular size markers are indicated to the left of (A) and (B) in kilodaltons.

Department of Biology, University of California at San Diego, La Jolla, CA 92093.

*To whom correspondence should be addressed.

critical concentration of assembly for the mutant protein was approximately 75 μg/ml, and the apparent efficiency of assembly was approximately the same as that found for the wild-type protein. However, the mutant protein failed to form filaments during dialysis at 37°C (Fig. 3D). Filaments formed of the mutant (or wild-type) protein at 4°C were stable when incubated at 37°C (*12*). These results indicate that assembly of filaments by the mutant protein in vitro is temperature-sensitive although the maintenance of filament structure is not.

Our results demonstrate that MDM1 is an intermediate filament–forming protein of yeast. MDM1 assembles into intermediate filaments in vitro under conditions very similar to those used for filament formation by the mammalian proteins vimentin and desmin (*17*). Although yeast and all eukaryotic cells have well-characterized microfilament (actin-based) and microtubule (tubulin-based) cytoskeletons (*18–20*) as well as nuclear lamins (*21*), cytoplasmic intermediate filament networks have not been readily apparent in yeast (*4*). A ring of 10-nm filaments in the mother-bud neck of yeast cells has been described previously (*22, 23*); however, evidence for a relation between these structures and intermediate filament networks of animal cells is lacking. The MDM1-containing structures, which extend throughout the cytoplasm (*7*), are likely to represent a cytoskeletal network related to the intermediate filament systems of higher eukaryotic cells. The punctate structures observed by indirect immunofluorescence (*7*) may coincide with junctions or organizing centers connected by individual MDM1 filaments (which are undetectable by currently available methods), or additional, distinct proteins may constitute filamentous connections along the punctate arrays. Although the structural details of this network remain to be clarified, the presence of an intermediate filament–like protein in yeast suggests that such polypeptides are universal constituents of all eukaryotic cells.

The *mdm1* mutation prevents the assembly of intermediate filaments at 37°C in vitro. The behavior of the purified protein parallels the in vivo phenotype of the *mdm1* mutant cells in which the punctate, MDM1-containing structures disappear 30 to 60 min after the cells are shifted to 37°C (*7, 12*). This time lag suggests that filaments readily turn over and that there is a block in new assembly rather than the temperature lability of preexisting structures.

The effect of the single *mdm1* lesion (Asn for Ser) suggests that this amino acid change occurs in a domain essential for assembly. The residues of vimentin and cytokeratin that correspond by sequence alignment (*7*) to the mutated amino acid lie in a conserved "linking" domain (termed L12) that joins the two halves of the central α-helical rod domain, a conserved structural feature of intermediate filament proteins (*4*). Our results may suggest a role for this domain in facilitating intermediate filament formation.

The temperature-sensitive defects in nuclear and mitochondrial inheritance and the positioning of the mitotic spindle in the *mdm1* mutant (*8*) indicate the cellular functions of the MDM1 protein. The MDM1-containing structures in the cell may constitute a network or matrix that serves both to mediate organelle transfer into develop-

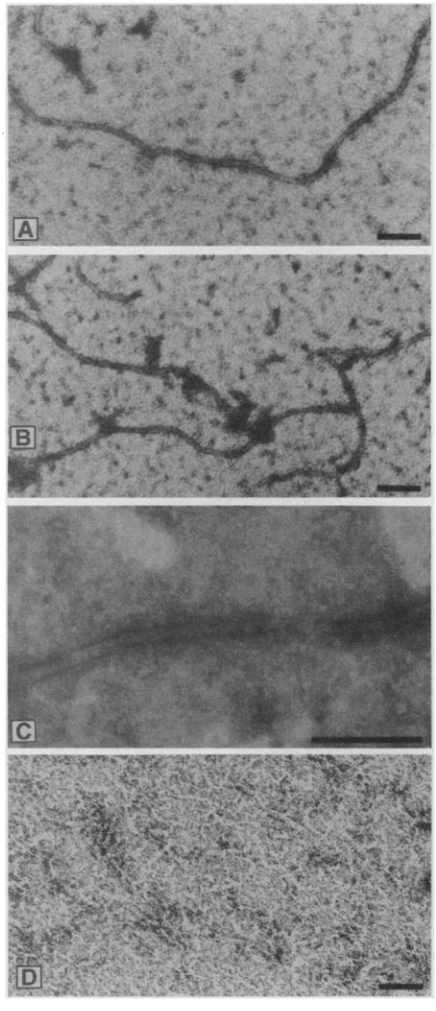

Fig. 2. Filament formation by purified MDM1 protein in vitro. (**A** and **B**) Electron micrographs of negatively stained (uranyl acetate) filaments formed by dialysis against PBS. (**C**) Enlarged electron micrograph of filament formed by dialysis against PBS and stained with phosphotungstic acid. (**D**) Electron micrograph of MDM1 sample dialyzed against low ionic strength buffer. The protein concentration for all samples before dialysis was 0.2 mg/ml. Bars represent 100 nm.

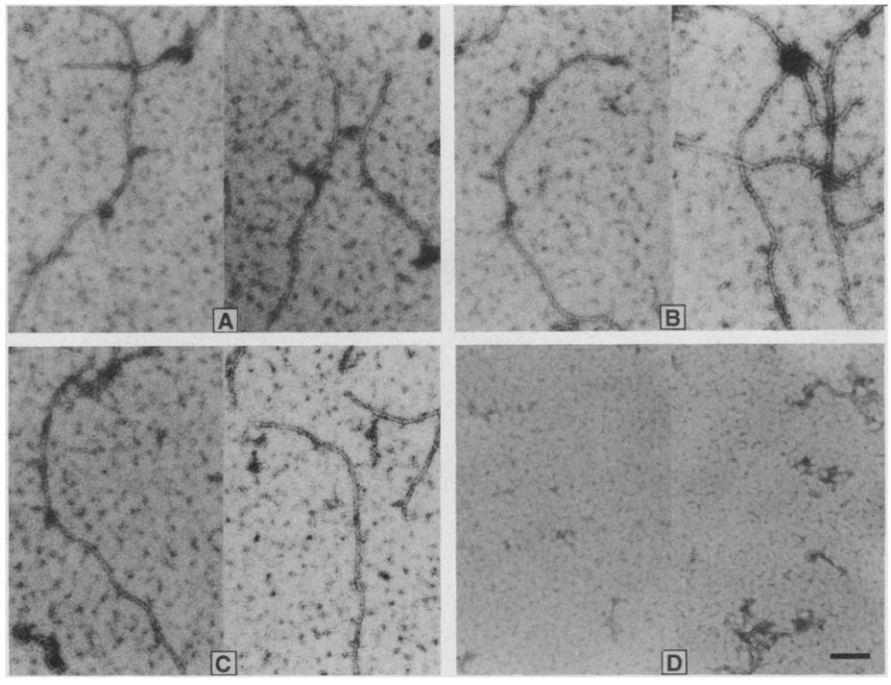

Fig. 3. Effect of temperature on filament assembly by wild-type or mutant MDM1 proteins. Samples (protein concentration of 0.2 mg/ml) were dialyzed against PBS at 4°C or 37°C, placed on carbon-coated specimen grids, and stained with uranyl acetate. Shown are two representative samples for each dialysis condition. (**A**) Electron micrographs of wild-type protein dialyzed at 4°C. (**B**) Electron micrographs of wild-type protein dialyzed at 37°C. (**C**) Electron micrographs of mutant protein dialyzed at 4°C. (**D**) Electron micrographs of mutant protein dialyzed at 37°C. All samples are shown at the same magnification. Bar represents 100 nm.

ing buds and to orient the mitotic spindle. These functions are consistent with earlier proposals that intermediate filaments organize cytoplasmic space (*1*) and mediate organelle distribution (*24*).

REFERENCES AND NOTES

1. E. Lazarides, *Nature* **283**, 249 (1980).
2. O. Skalli and R. D. Goldman, *Cell Motil. Cytoskeleton* **19**, 67 (1991).
3. N. Geisler and K. Weber, *EMBO J.* **1**, 1649 (1982).
4. P. M. Steinert and D. R. Roop, *Annu. Rev. Biochem.* **57**, 593 (1988).
5. R. D. Goldman, R. V. Zackroff, P. M. Steinert, in *Cellular and Molecular Biology of Intermediate Filaments*, R. D. Goldman and P. M. Steinert, Eds. (Plenum, New York, 1990), pp. 3–17.
6. E. Fuchs, *Curr. Biol.* **1**, 284 (1991).
7. S. J. McConnell and M. P. Yaffe, *J. Cell Biol.* **118**, 385 (1992).
8. S. J. McConnell, L. C. Stewart, A. Talin, M. P. Yaffe, *ibid.* **111**, 967 (1990).
9. To recover the mutant *mdm1* gene, we isolated from plasmid YIp5 (MDM1) (*7*) a 1.7-kb Eco RV–Xba I fragment containing sequences from a chromosomal region located 3′ to *MDM1* and cloned it into the Bam HI site of plasmid YIp5 (*25*). The resulting plasmid (YIp5-XR) was linearized with Kpn I and transformed into yeast strain MYY403 (*MAT*a, *leu2*, *his3*, *ura3*, *mdm1*). Chromosomal DNA prepared from stable transformants was digested with Sal I, treated with T4-DNA ligase to circularize the fragments, and transformed into *Escherichia coli* (DH5α). Plasmids isolated from transformants were shown by restriction mapping to contain the *mdm1* gene, and the nucleotide sequence of the mutant gene was determined by dideoxy sequencing (*11*). To test genetic complementation by the mutant gene, we cloned a 4.5-kb fragment that contained the entire *mdm1* gene into the yeast shuttle vector YCp50 (*26*), and the resulting plasmid was transformed into yeast strain MYY403.
10. R. Rothstein, *Methods Enzymol.* **194**, 281 (1991).
11. F. Sanger, S. Nicklen, A. R. Coulson, *Proc. Natl. Acad. Sci. U.S.A.* **74**, 5463 (1977).
12. S. J. McConnell and M. P. Yaffe, unpublished data.
13. A unique Nde I site was created at the initiator methionine of the *MDM1* gene (*7*) with the MutaGene M13 in vitro Mutagenesis Kit (Bio-Rad). This site allowed the isolation of a 1519-bp Nde I–Nhe I fragment containing the entire *MDM1* gene, which was cloned into the pET11-a vector (*27*) to create plasmid pET11-a-*MDM1*. We constructed a bacterial expression vector containing the mutant gene (pET11-a-*mdm1*) by replacing the Stu I–Nhe I fragment in plasmid pET11-a-*MDM1* with the corresponding sequence from the cloned *mdm1* gene. Wild-type and mutant forms of MDM1 were expressed in *E. coli* strain BL21(DE3)pLysS and purified from inclusion bodies as described (*14*), except that leupeptin and pepstatin A were added to extraction buffers to a final concentration of 1 mg/liter, and final extracts were clarified by centrifugation at 16,000*g* for 1 min. Protein concentrations were determined with the use of the bicinchoninic acid protein assay reagent (Pierce). The purity of wild-type and mutant MDM1 was analyzed by SDS–polyacrylamide gel electrophoresis followed by Coomassie staining or immunoblotting.
14. A. Domingo, A. J. Sarriá, R. M. Evans, M. W. Klymkowsky, in *The Cytoskeleton, A Practical Approach*, K. L. Carraway and C. A. C. Carraway, Eds. (IRL Press, Oxford, 1992), pp. 223–255.
15. MDM1 protein solubilized in 9 M urea was dialyzed against either phosphate-buffered saline (PBS) [0.14 M NaCl, 3 mM KCl, 8 mM Na_2HPO_4, 1.5 mM KH_2PO_4, 1 mM dithiothreitol (DTT), and 0.1 mM phenylmethylsulfonyl fluoride (PMSF) (pH 7.3)] or low ionic strength buffer (2 mM tris HCl, pH 7.5, 1 mM DTT, and 0.1 mM PMSF) for 16 to 20 hours. Suspensions of dialyzed proteins were placed on carbon-coated specimen grids for 1 min, excess solution was removed, and the grids were treated with 1% uranyl acetate or 1% aqueous phosphotungstic acid for 1 min.
16. Efficiency of filament formation, as defined previously (*28*), was determined by differential centrifugation and analysis of fractions by electron microscopy. The dialysate was centrifuged at 16,000*g* for 2 min. The pellet contained 50 to 75% of the total MDM1 and appeared as clumps and nonfilamentous aggregrates by electron microscopy. The supernatant (25 to 50% of the total protein) contained numerous filaments. When this latter material was centrifuged at 250,000*g* for 1 hour, at least 80% (20 to 40% of the total protein) was found in the pellet and appeared as filaments and filamentous aggregrates in the electron microscope.
17. P. Steinert, R. Zackroff, M. Aynardi-Whitman, R. D. Goldman, *Methods Cell Biol.* **24**, 399 (1982).
18. J. V. Kilmartin and A. E. M. Adams, *J. Cell Biol.* **98**, 922 (1984).
19. A. E. M. Adams and J. R. Pringle, *ibid.*, p. 934.
20. J. H. Thomas, P. Novick, D. Botstein, in *Molecular Biology of the Cytoskeleton*, G. G. Borisy, D. W. Cleveland, D. B. Murphy, Eds. (Cold Spring Harbor Laboratory, Cold Spring Harbor, NY, 1984), pp. 153–174.
21. S. D. Georgatos, I. Maroulakou, G. Blobel, *J. Cell Biol.* **108**, 2069 (1989).
22. B. Byers and L. Goetsch, *ibid.* **69**, 717 (1976).
23. H. B. Kim, B. K. Haarer, J. R. Pringle, *ibid.* **112**, 535 (1991).
24. E. Wang and R. D. Goldman, *ibid.* **79**, 708 (1978).
25. K. Struhl, D. T. Stinchcomb, S. Scherer, R. W. Davis, *Proc. Natl. Acad. Sci. U.S.A.* **76**, 1035 (1979).
26. M. D. Rose, P. Novick, J. H. Thomas, D. Botstein, G. R. Fink, *Gene* **60**, 237 (1987).
27. F. W. Studier, A. H. Rosenberg, J. J. Dunn, J. W. Dubendorff, *Methods Enzymol.* **185**, 60 (1990).
28. A. K. Wilson, P. A. Coulombe, E. Fuchs, *J. Cell Biol.* **119**, 401 (1992).

29. We thank L. Washington for assistance with electron microscopy, A. Domingo and M. Klymkowsky for advice on expression and purification of intermediate filament proteins from bacteria, and J. Singer, D. Forbes, and V. Malhotra for suggestions and reading of the manuscript. Supported by NSF grant MCB-9004719.

2 October 1992; accepted 19 February 1993

Rapid Loss of CD4$^+$ T Cells in Human-PBL-SCID Mice by Noncytopathic HIV Isolates

Donald E. Mosier, Richard J. Gulizia, Paul D. MacIsaac, Bruce E. Torbett, Jay A. Levy

Human immunodeficiency virus (HIV) isolates differ in cell tropism, replication, pathogenicity, and syncytial induction in vitro. CD4$^+$ T cells were enumerated in severe combined immunodeficient mice transplanted with human peripheral blood leukocytes (hu-PBL-SCID mice) and infected with HIV isolates with different in vitro cytopathicity. Two noncytopathic, macrophage-tropic strains, HIV-1_{SF162} and HIV-2_{UC1}, induced extensive CD4$^+$ T cell depletion, whereas HIV-1_{SF33}, which is highly cytopathic for T cells in vitro, caused little CD4$^+$ T cell depletion at equivalent virus burden. In vitro cytopathicity assays therefore do not predict CD4 depletion in the hu-PBL-SCID model.

The central immunologic defect after infection with HIV-1 is the decline in CD4$^+$ T lymphocytes, which precedes the progression from asymptomatic infection to the acquired immunodeficiency syndrome (AIDS). The duration of this process is usually greater than a decade, and an animal model with accelerated CD4$^+$ T cell depletion would be useful for investigating the mechanism of pathogenesis in vivo (*1*). The simplest model for CD4$^+$ T cell loss would be a direct, cytopathic infection of cells by HIV. However, some isolates of HIV-1 show no cytopathic effect on cultured human T cells and yet have been recovered from patients with CD4$^+$ T cell depletion (*2*). These observations have suggested that HIV-1 infection leads to dysfunction and eventual loss of CD4$^+$ T cells by indirect mechanisms that do not require virus infection of the target cell. Understanding such mechanisms of pathogenesis is also made difficult by the extensive biologic and genetic diversity of HIV-1 or HIV-2 isolates (*2–4*). HIV isolates differ in their cell tropism, cytopathicity, ability to induce syncytia, and rate of replication (*4–11*). Several of these properties are related to changes in the *env* gene encoding the gp120 envelope glycoprotein (*12–20*). It would aid our understanding of AIDS pathogenesis if these changes in the behavior of HIV in vitro could be related to the process of CD4$^+$ T cell depletion in vivo.

To address these issues, we have studied the fate of human CD4$^+$ T cells in severe combined immunodeficient mice reconstituted with adult human peripheral blood mononuclear leukocytes (hu-PBL-SCID mice) and infected with several well-characterized HIV-1 viruses and one HIV-2 strain. The human T cells (including both CD4$^+$ and CD8$^+$ T cells and CD45RO$^+$

D. E. Mosier, R. J. Gulizia, B. E. Torbett, Department of Immunology, Scripps Research Institute, La Jolla, CA 92037.
P. D. MacIsaac, Medical Biology Institute, La Jolla, CA 92037.
J. A. Levy, Department of Medicine, Cancer Research Institute, University of California School of Medicine, San Francisco, CA 94143.